arXiv:1006.3220v1 [physics.ins-det] 16 Jun 2010

A Lightweight Field Cage for a Large TPC Prototype for the ILC

Ties Behnke, Klaus Dehmelt, Ralf Diener, Lea Hallermann, Takeshi Matsuda, Volker Prahl, Peter Schade

DESY, Hamburg, Germany

June 17, 2010

Abstract

We have developed and constructed the field cage of a prototype Time Projection Chamber for research and development studies for a detector at the International Linear Collider. This prototype has an inner diameter of 72 cm and a length of 61 cm. The design of the field cage wall was optimized for a low material budget of 1.21% of a radiation length and a drift field homogeneity of $\Delta E/E \lesssim 10^{-4}$. Since November 2008 the prototype has been part of a comprehensive test beam setup at DESY and used as a test chamber for the development of Micro Pattern Gas Detector based readout devices.

1 Introduction

A Time Projection Chamber (TPC) is planned as the main tracking detector for the International Large Detector, ILD, a proposed detector for the International Linear Collider, ILC [1]. This TPC will be confronted with multi-jet events with high track multiplicities. It has to provide a very high tracking efficiency and precision while maintaining robustness towards machine backgrounds. The detailed performance requirements for the ILD TPC are summarized in the ILD Letter of Intent [2] and shown in Table 1.

The momentum resolution goal is $\delta(1/p_\perp) \approx 9 \times 10^{-5}\,\mathrm{GeV}^{-1}$ for the TPC alone and derived from requirements on the physics performance of the ILD detector. This is directly linked with the point resolution of the TPC which should be better than 100 µm in the $r\varphi$ plane, perpendicular to the beam pipe. Of particular importance for the operation of the TPC will be the minimization of the material budget of the field cage structure. A low material budget is essential to suppress conversion and multiple scattering processes before particles reach the calorimeter.

Size	inner field cage ∅: 0.65 m
	outer field cage ∅: 3.6 m
	total length: 4.3 m
point resolution in $r\varphi$	$\sigma_\perp < 100\,\mu$m modulo φ
point resolution in z	$\sigma_z < 0.5$ mm modulo θ
2-hit resolution in $r\varphi$	~ 2 mm (modulo track angles)
2-hit resolution in z	~ 6 mm (modulo track angles)
momentum res.	$\delta(1/p_\perp) \approx 9 \cdot 10^{-5}\,\mathrm{GeV}^{-1}$
$\mathrm{d}E/\mathrm{d}x$ resolution	$\sim 5\,\%$
TPC material budget	$\lesssim 0.01\,\mathrm{X}_0$ of the inner barrel
	$\lesssim 0.04\,\mathrm{X}_0$ to the outer barrel
	$\lesssim 0.15\,\mathrm{X}_0$ to the end caps
efficiency (TPC alone)	$> 97\,\%$ (for $p_\perp > 1\,\mathrm{GeV/c}$)

Table 1: *Design goals for the ILD TPC* [2].

The performance goals significantly exceed the corresponding numbers reached by prior TPCs in collider experiments (e.g. [3, 4, 5]).

During the last few years, Micro Pattern Gas Detector (MPGD) amplification systems were under study within the LCTPC collaboration [6] for the readout of the ILD TPC. The investigated MPGDs are Gas Electron Multiplier (GEM) [7] and Micromegas [8] in combination with a pad or pixel readout system. Both, GEMs or Micromegas devices can be mounted on a lightweight support and allow for the construction of a TPC end plate with a low material budget. In addition, they provide a flat and homogeneous surface without large $\vec{E} \times \vec{B}$ effects in the vicinity of the readout plane.

First feasibility studies for a GEM or Micromegas based TPC readout were carried out by several research groups. The studied readout structures had sizes of typically 10 cm × 10 cm (e.g. [2] and references therein).

The next step is to demonstrate a TPC with several prototype readout modules in a strong magnetic field. A test beam infrastructure for the studies planned was realized at DESY in the framework of the EUDET project [9]. The setup provides a superconducting solenoid magnet with a bore diameter of 85 cm, a usable length of about 1 m and a magnetic field strength of up to 1.25 T. The TPC Prototype has an outer diameter of 77 cm and a length of 61 cm (Fig. 1 and Fig. 2) and is dimensioned to be operated inside the magnet.

The diameter of this Large TPC Prototype (LP) is similar to the inner field cage of the ILD TPC. Moreover, the ratio L/B of the TPC drift distance L to the magnetic field strength B is the same for the LP ($B = 1\,\mathrm{T}$, $L = 60\,\mathrm{cm}$) and the ILD TPC ($B = 3.5\,\mathrm{T}$, $L = 215\,\mathrm{cm}$). If this ratio remains constant, the magnitude of acceptable electric field inhomogeneities inside the TPC drift volume will also remain the same. Therefore, the relative

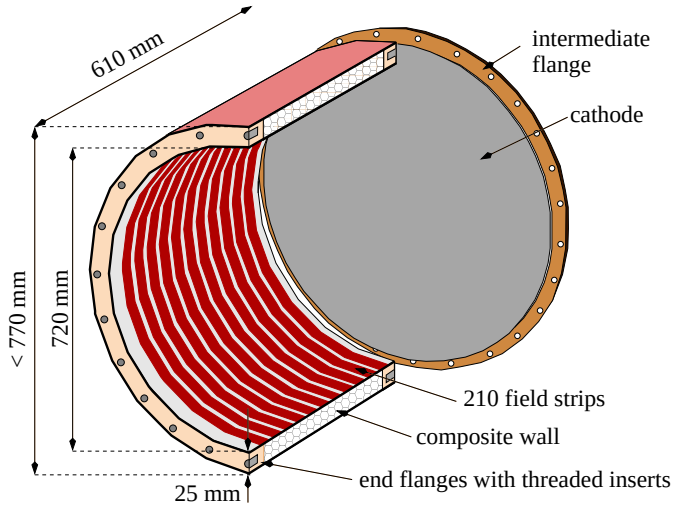

Figure 1: *Overview of the design of the field cage: Complementary to the field cage barrel, a cathode end plate was constructed. The cathode is supported inside the field cage by an intermediate flange.*

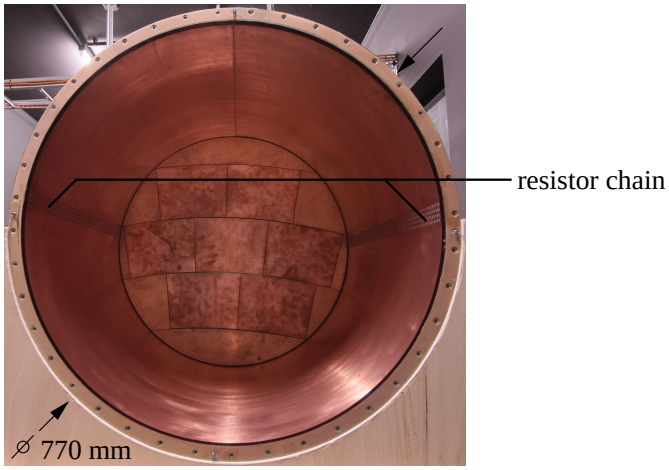

Figure 2: *View into the field cage from the cathode side: The anode is assembled with an end plate, which was constructed within the LCTPC collaboration* [6]. *Two resistor chains are installed on the inside wall of the barrel and interconnect the field strips.*

mechanical accuracy specifications are similar for the LP and the ILD TPC.

In the following, optimization studies for the LP field cage and its construction are discussed. Based on the experience gained with the LP a preliminary design for the ILD TPC field cage wall is proposed.

2 Requirements for the Field Cage

The design of the Large TPC Prototype was optimized towards a low material budget of the walls, a high homogeneity of the electric drift field and an adequate maximum operational voltage.

The material budget per wall of the barrel was required to be close to the design goal of $1\%\,X_0$ for the ILD TPC.

Radial components ΔE_r of the electric drift field inside the LP volume should not exceed $\Delta E_r/E \lesssim 10^{-4}$. This limits systematic effects on the resolution due to field inhomogeneities to less than 30 µm. Controlling the field distortions on a level of 10^{-4} requires a mechanical accuracy of the field cage in the 100-µm regime.

The LP has to allow for operations with various gases with an overpressure of up to 10 mbar. Deformations of the structure due to the overpressure should stay below 100 µm. The anticipated maximum drift fields are in the range of 350 V/cm, which require long term operations without voltage breakdowns with 20 kV permanently applied to the cathode of the LP.

3 Design of the Wall Structure

The field cage barrel of the LP was built as a lightweight sandwich structure. The wall consists of a 23.5-mm thick over-expanded aramid honeycomb material (Fig. 3(a)) which is embedded between two layers of glass-fiber reinforced plastic (GRP) and a polyimide layer for electrical insulation.

A low material budget of the wall was achieved by minimizing the thickness of the GRP layers. The wall was tested for mechanical robustness and high voltage stability.

3.1 Mechanical Robustness

To test the mechanical properties of the field cage wall, several sample pieces were produced (Fig. 3). Two sample pieces were subjected to a four point bending test (Fig. 4)[1]. For small forces F, the observed bending s rises linear with the applied force F according to

$$\frac{\mathrm{d}s}{\mathrm{d}F} = 11.1 \pm 0.1\,\frac{\mu\mathrm{m}}{\mathrm{N}} \quad (F < 100\,\mathrm{N}).$$

To limit the deflection s to below 100 µm, the force F on the structure must not exceed 10 N. This corresponds to a maximum pressure of 5 mbar on the sample. At larger forces the samples suffer from partial delamination and are irreversibly damaged.

[1] The tests were performed in cooperation with the Technical University of Hamburg-Harburg.

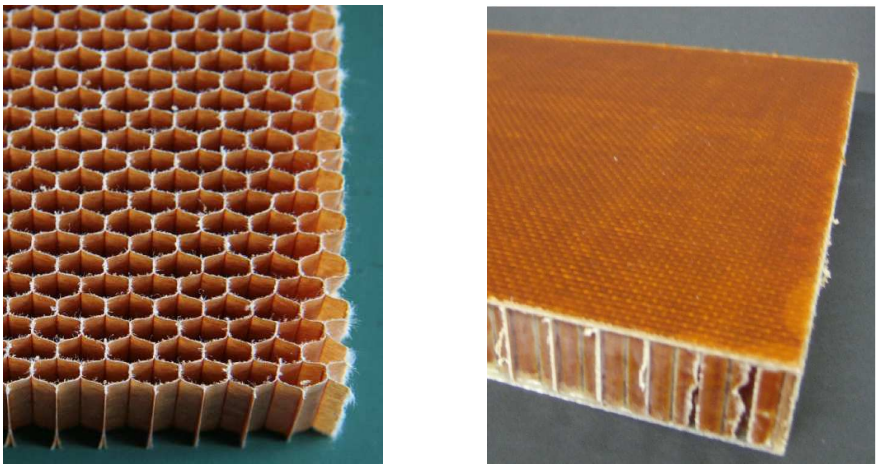

(a) honeycomb material (b) wall sample

Figure 3: *Composite wall structure: (a) Over-expanded honeycomb was used for the construction of the LP wall. The cells of this material are expanded in one direction and have an almost rectangular shape. The modified cell structure increases the flexibility of the material perpendicular to the direction of the expansion and allows for the construction of cylindrical structures. (b) Sample piece of the wall, as used for mechanical and electrical tests with* 400 µm *thick GRP layers.*

Translated from the flat geometry of the test setup to the cylindrical structure of the LP, the bending of the barrel is reduced by a factor of approximately 80. The factor was determined in FEM calculations. To keep the wall deflection below 100 µm, the overpressure inside the LP should not exceed 400 mbar. Thus, the field cage barrel is mechanically robust for operations at the envisaged overpressure of 10 mbar.

3.2 High Voltage Stability

To guarantee the operational safety, high-voltage breakdown tests were performed. For this purpose, the wall samples were installed in air between a parallel plate capacitor and 30 kV applied for 24 h.

The samples evaluated contained polyimide insulation layers with thicknesses between 50 µm and 150 µm. No breakdowns were observed.

The final design of the LP wall contains a polyimide insulation layer of 125 µm thickness and the LP is expected to be high-voltage stable for long term operations with voltages of 20 kV.

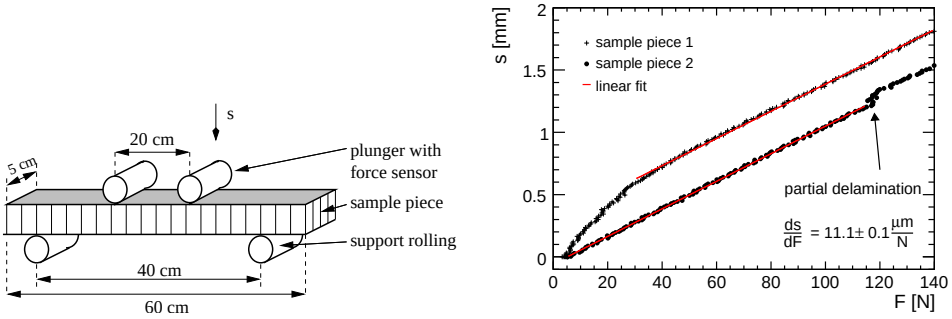

(a) four-point bending test setup (b) test results for two sample pieces

Figure 4: *Four-point bending test: (a) In the test setup, the pieces rest on two rollings with a distance of* 40 cm *while two similar rollings in a distance of* 20 cm *press centrally against the sample. (b) The applied force F and the elongation s are measured in parallel. The dependence $s(F)$ is linear with an equal slope for both samples. In case of the first sample the linear range starts only at forces of about* 40 *N due to an improper preparation of the measurement apparatus. The second sample suffers from first damage at forces of about 120 N (partial delamination).*

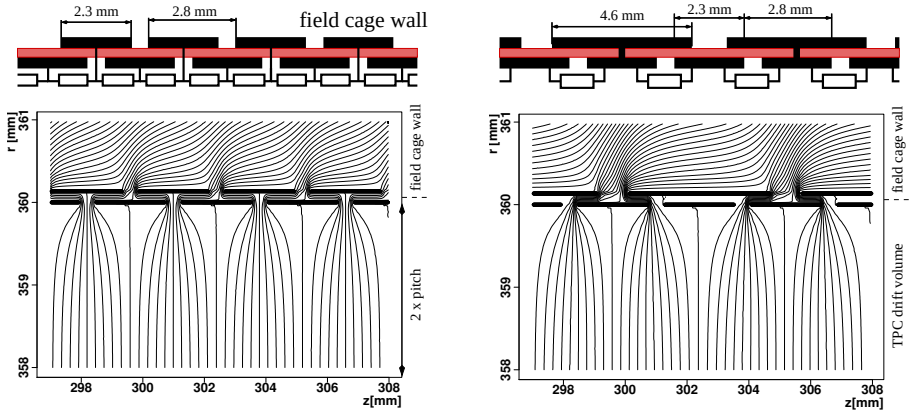

(a) displaced mirror strips, lying on the intermediate potential of the two adjacent field strips

(b) large mirror strips, directly connected to the field strips

Figure 5: *Calculated electric equipotential lines on the inner wall of the field cage: (a) A standard layout with displaced mirror strips covering the gaps between the field strips. (b) A layout with extended mirror strips.*

4 Design of the Field Forming Elements

The inside of the LP barrel is covered with conductive copper rings (see Fig. 1 and Fig. 2). These field shaping strips lie on stepwise decreasing

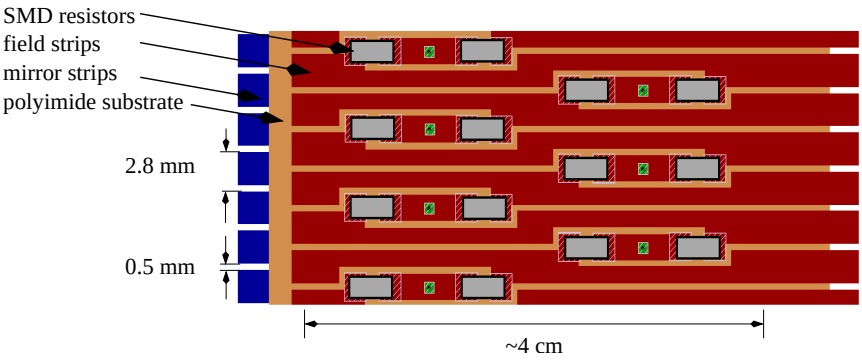

Figure 6: *Layout of the resistor chains on the field strip boards for the LP: Two neighboring strips are connected by two surface mount (SMD) resistors via an intermediate connection which tabs through the board to the mirror strip. This corresponds to the strip design shown in Figure 5(a).*

potentials from the anode to the cathode and define the boundary condition for the electric field along the inside of the TPC barrel. A second layer, the mirror strips, is installed directly under the field strips. Each mirror strip covers the gap between two field strips in front. Together, the two layers provide a shielding against external electrical influences on the internal field.

With the help of finite-element field calculations several strip arrangements were investigated. The layout chosen for the LP (Fig. 5(a)) is a typical arrangement used in TPCs (e.g. [10]). The field shaping strips have a pitch of 2.8 mm and are intersected by 0.5 mm gaps, while the mirror strips are a copy of the field strips but displaced by half the pitch. Each mirror strip lies on the intermediate potential of the two adjacent field strips. These potentials are applied by a resistor chain. If the insulation layer between the field strips and the mirror strips is kept thin compared to the strip's width, field distortions occur only in a narrow band with a thickness of two times the pitch along the inner field cage wall.

A second design was evaluated as an alternative (Fig. 5(b)). Here, only every second field strip is connected to a mirror strip while each mirror strip covers two gaps. As a result, the drift field becomes homogeneous at a distance of three times the pitch from the wall. This arrangement would allow for a simpler design of the resistor chain.

In the LP, the strip design is realized on a 61 cm × 226 cm large flexible printed circuit board – the width and length of the board correspond to the length and inner circumference of the field cage, respectively. The board consists of a 75-µm thick polyimide carrier foil with 35-µm thick copper field and mirror strips on either side, respectively. The side with the field strips accommodates places to solder surface-mount resistors (Fig. 6). Two of these resistor chains are installed on the inside wall of the field cage, in diametrical opposite positions (see Fig. 2).

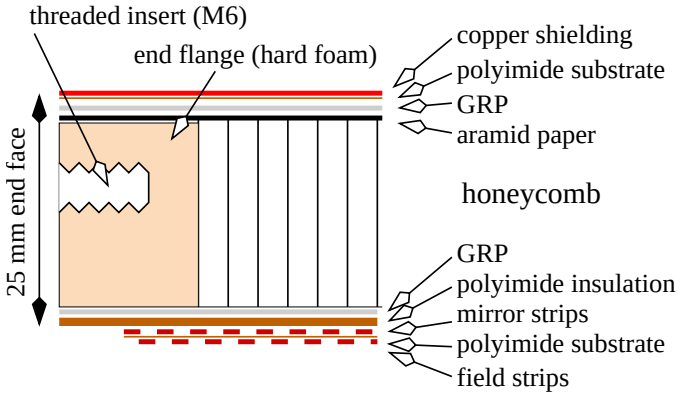

Figure 7: *Cross section of the Large Prototype field cage wall.*

insulation layer	DuPont™, Kapton® 500HN
aramid honeycomb	Hexel, HexWeb®
	HRH 10/OX-3/16-1.8
hard foam end flanges	SP, Corecell™ S-Foam
aramid paper	DuPont™, Nomex® 410

Table 2: *Materials used for the construction of the field cage.*

For technical reasons, the final 61-cm wide board was split up into two pieces. These two half-boards were produced by industry[2] and afterwards combined into one piece.

The field strip board was assembled with resistors and electrically tested prior to the construction of the field cage. It is equipped with 1 MΩ resistors with a measured spread of $\Delta R \lesssim 100\,\Omega$, or $\Delta R/R \lesssim 10^{-4}$. The installation of the field strip board into the field cage is described in Section 7.

5 Cross Section of the Field Cage Wall

The wall of the field cage consists of four main components. Figure 7 displays the cross section in detail and Table 2 summarizes the materials used in the wall laminate.

An electrical shielding layer on the outside of the barrel is realized by a layer of 10 µm thick copper on a polyimide carrier of 50 µm thickness. The copper layer is electrically grounded and confines the electric field of the TPC to the inside of the field cage.

The bulk of the wall consists of the honeycomb spacer material sandwiched between two GRP layers. The honeycomb is 23.5 mm thick and

[2]Optiprint, Innovative PCB Solutions, http://www.optiprint.ch

layer of the wall	d [cm]	X_0 [cm]	d/X_0 [%]
copper shielding	0.001	1.45	0.07
polyimide substrate	0.005	32.65	0.02
outer GRP	0.03	15.79	0.19
aramid paper	0.007	29.6	0.02
honeycomb	2.35	1383	0.17
inner GRP	0.03	15.79	0.19
polyimide insulation	0.0125	32.65	0.04
mirror strips	$0.8 \cdot 0.0035$	1.45	0.19
polyimide substrate	0.0050	32.65	0.02
field strips	$0.8 \cdot 0.0035$	1.45	0.19
epoxy glue	$\approx 6 \cdot 0.007$	≈ 35.2	0.12
		$\sum$	1.21

Table 3: *Composition and radiation lengths of the materials in the field cage wall: the thickness of the different layers were derived from the specifications of the used materials. Material densities and radiation lengths were taken from* [11]. *The thickness of the copper layers are reduced by factors of 0.8 because the field strips cover only* 80% *of the inner field cage barrel.*

has a density of $29\,\mathrm{kg/m^3}$. A layer of aramid paper was introduced on the outside of the honeycomb for constructional reasons (see Sec. 7).

A 125-µm thick polyimide layer ensures the high-voltage stability of the wall. This polyimide layer alone has a breakdown voltage of about 20 kV. The honeycomb sandwich is non conductive and contributes further to the high voltage stability of the wall laminate.

The field and mirror strips, on the inside of the barrel (see Fig. 5(a)) suppress the influence of the ground potential of the outer shielding on the drift field and guarantee an electric field homogeneity of $\Delta E/E \lesssim 10^{-4}$.

The field cage wall is terminated on the anode and cathode side by end flanges made of hard foam (see Tab. 2). These flanges have a height of 23.5 mm, which matches the height of the honeycomb material, and are populated with threaded stainless steel inserts for the attachment of the anode and cathode end plates.

The radiation length of the wall is

$$X^{\mathrm{wall}} = 1.21 \pm 0.10\,\% X_0.$$

In the calculation of X^{wall} (Tab. 3), GRP was assumed to consist of 2/3 glass fiber and 1/3 epoxy glue. In addition, the thickness of the epoxy layers used to glue together the different layers of the wall was estimated to be $70 \pm 30\,\mu\mathrm{m}$ thick each.

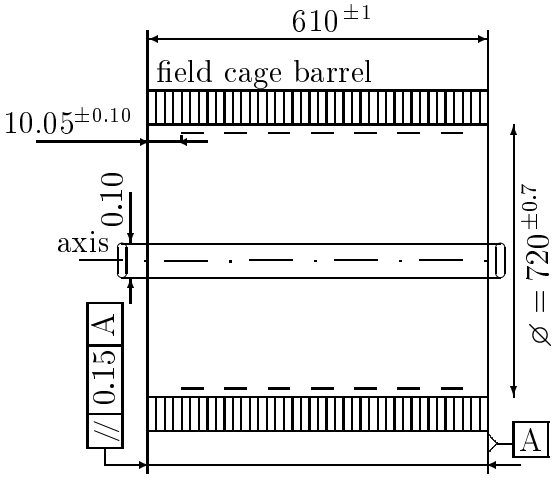

Figure 8: *Mechanical accuracy specifications for the field cage: The end flanges were required to be parallel with deviations less than* 150 µm. *The nominal axis of the field cage is defined as perpendicular to the anode end face in the center of the field cage. The measured axis of the field cage is specified to be within a tube with a diameter of* 100 µm *with respect to the reference axis over the whole length of the field cage. The distance of the first field strip to the anode end face was specified to be* 10.05 ± 0.10 mm.

6 Specification of Mechanical Accuracy

Detailed tolerance specifications for the field cage (Fig. 8) were derived from a study of field quality degradation due to an imperfect chamber geometry and the impact on the achievable point resolution [12].

Most critical is the correct alignment of the field cage axis relative to the anode end flanges. A misalignment of the axis produces a sheared field cage. This causes radial components of the electric field which deteriorate the point resolution in the $r\varphi$ plane. Therefore the tolerance on the alignment of the axis relative to the normal of the anode end face is defined most stringently to be within 100 µm.

Less critical is the parallel alignment of the anode relative to the cathode. A misalignment produces mainly field deviations along the z-axis and to a lesser degree in the radial direction. Hence the parallel alignment of the cathode relative to the anode was defined less stringently and required to be precise within 150 µm.

The length of the field cage is not a critical parameter because it can be adjusted by positioning the cathode inside the field cage. Therefore the specification has a comparably large tolerance of 1 mm. Similarly, the field cage diameter has a larger tolerance and is dimensioned to be 720.0 ± 0.3 mm.

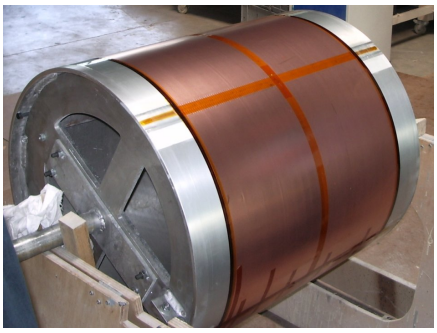

(a) mandrel assembled with field strip board

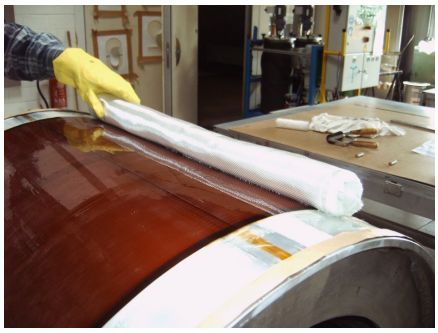

(b) lamination of the inner GRP layer

Figure 9: *Construction of the field cage on a mandrel.*

7 Production of the Field Cage Barrel

The field cage was manufactured[3] over a forming tool which served as a mold. This was a 75-cm long mandrel with a diameter of 72 cm – according to the field cage's inner diameter. The mandrel could be reduced in diameter by a few millimeter via an expansion slot.

In the first step of the production, the field strip board was positioned on the mandrel (Fig. 9(a)). Two 1-mm deep slots had been machined into the mandrel surface to accommodate the resistors on the field strip board. Then, the different layers of the field cage wall were laminated onto the foil. For the production of the GRP, first a glass-fiber canvas was put onto the mandrel (Fig. 9(b)) and moisturized with epoxy glue. Afterwards, air inclusions were removed from the layer with an underpressure treatment and the epoxy cured at 60 °C. The curing temperature was kept as low as possible to reduce thermal stresses on the field cage.

In the following steps of the production, the pre-produced end flanges and the honeycomb were laminated onto the inner GRP layer. On top, a layer of aramid paper sealed the cells of the honeycomb (see Fig. 7). A direct lamination of the outer GRP layer onto the open honeycomb could have filled the cells with epoxy and caused a higher and inhomogeneous material buildup of the wall. The shielding layer of copper loaded polyimide completed the field cage.

With the lamination finished, the surfaces of the end flanges were machined for flatness and parallelism. Finally the mandrel was reduced in diameter and removed from the field cage.

[3]DESY in cooperation with Haindl, individuelle Kunststoffverbundbauweise, http://www.haindl-kunststoff.de

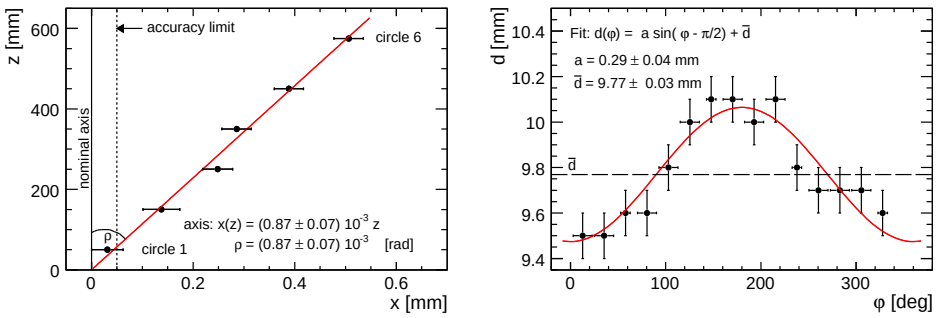

(a) center points of circles fitted to reference points taken on the inside of the barrel

(b) distance of the first strip to the anode end face

Figure 10: *Determination of the field cage axis: The axis of the chamber is tilted and reaches an offset of* 500 µm *at the cathode. The coordinates* z, r *and* φ *define a cylindrical coordinate system for the field cage, with* z *pointing in the direction of the nominal chamber axis, normal to the plane defined by the anode end face.* d *is the distance of the first field strip to the anode end face (Fig. 8).*

7.1 Production Quality Assurance

The important accuracy parameters for the field cage were surveyed in the commissioning phase of the LP at DESY. For this, about 100 measurement points were taken over the barrel with a spatial accuracy of 25 µm.

The end flanges of the field cage were found to be parallel with deviations below 40 µm, while the length of the field cage was measured to be 610.4 ± 0.1 mm. The diameter of the chamber was determined to 720.20 ± 0.07 mm over the whole length of the barrel. These numbers are in agreement with the specifications.

To determine the axis of the field cage, measurement points were taken on the barrel inside at six fixed distances relative to the anode reference plane. Each set of points defines a circle on the inside of the barrel and the center points of the six circles define the field cage axis. A tilt of the axis was found, which results in a maximum offset of 500 µm relative to the nominal position at the cathode (Fig. 10(a)). The angle between the measured axis and the nominal one was determined to be $\rho = 0.87 \pm 0.07$ mrad.

A second measurement of the axis was performed to confirm this result. For this, the distance d of the first field strip to the anode end face was determined at several places around the circumference. The field strips on the inside define parallel planes perpendicular to the field cage axis. Hence, d has a fixed value if the axis is aligned correctly.

However, the measured distance d varies sinus-like around the circumference (Fig. 10(b)). The amplitude of the sinus is 0.3 mm and equal to $\rho \cdot r_\mathrm{i}$. Here, $r_\mathrm{i} = 360$ mm is the inner radius of the LP and ρ the angle between

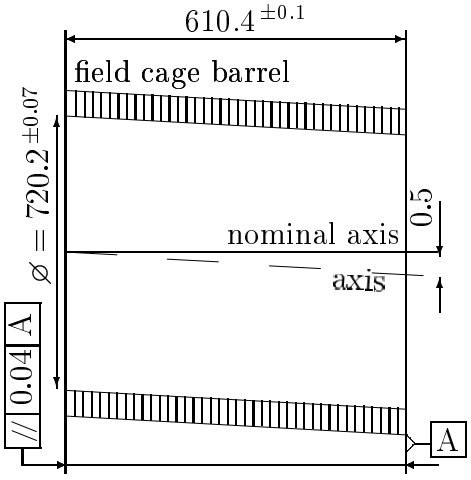

Figure 11: *Measured shape of the LP: The requirements in length, alignment of the end flanges and roundness of the barrel are fulfilled, but alignment of the field cage axis does not satisfy the accuracy goal.*

the measured and the nominal field cage axis determined with the initial method (Fig. 10(a)). Thus the amplitude has the expected magnitude, so that both methods agree on the misalignment of the axis.

Figure 11 illustrates the measured shape of the field cage. Due to the shear of the barrel, the electric drift field inside the chamber is not homogeneous to the required level (Fig. 12). The field inhomogeneities have a magnitude of $10^{-4} \leq \Delta E/E \lesssim 10^{-3}$.

8 Extrapolation to the ILD TPC

For the ILD, a TPC is planned with a diameter of the inner field cage of 65 cm, of the outer field cage of 360 cm and a drift distance of 215 cm. This is about 3.5 times longer than the LP. At the same time, the magnetic field of ILD is 3.5 T compared to 1 T for the LP. As mentioned in section 1, the ratio L/B of the magnetic field to the drift distance L is the same for both TPCs and so are the required relative mechanical accuracy specifications.

Scaling the mechanical tolerances of the LP by a factor of three yields a tolerance for the alignment of the field cage axis in the range of 300 µm and a required parallel alignment of anode and cathode of 450 µm for the ILD TPC.

The main challenge for the design of the ILD TPC will be the reduction of the material budget of the wall to 1% X_0 while increasing the high voltage stability to $\mathcal{O}(100\,\mathrm{kV})$.

Starting from the current LP wall cross section (see Fig. 7), a reduction of the material budget is possible by thinning down the field strips to 20 µm and

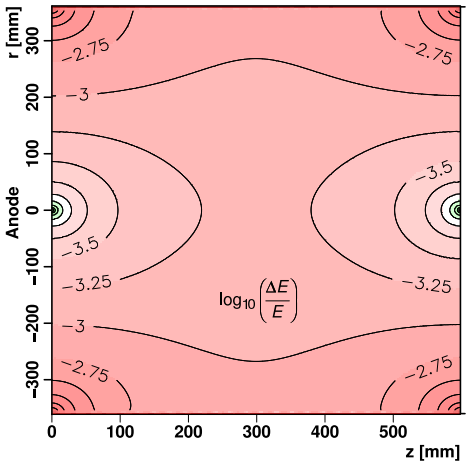

Figure 12: *Calculated field quality: Due to the shear of the field cage (see Fig. 11), the calculated electric field inside the LP is homogeneous only to a level of* $\Delta E/E \approx 10^{-3}$.

by replacing copper by aluminum. In addition, with further optimization studies of the chamber statics and mechanical tests, the thickness of the GRP could be diminished. This would reduce the contribution of epoxy and glass-fiber to the material budget. Assuming a moderate optimization, GRP layers of 200 µm could be sufficiently stable to construct a self supporting tube of 4.3 m length for the inner field cage.

The LP wall samples were tested to be high voltage stable up to at least 30 kV. In the wall sample tested, a single polyimide layer of 50 µm was introduced which can withstand 10 kV alone. The insulating honeycomb-GRP structure increased the high voltage stability to above 30 kV.

Extrapolating to the ILD TPC, the wall of the inner field cage could have a cross section as shown in Figure 13. Here, an insulation which is equivalent to a single 300 µm thick polyimide layer together with the honeycomb sandwich provide a high voltage stability in the range of 70 kV. This wall has a material budget of 1% X_0, which is the design value. However, the detailed fabrication of the thicker polyimide layer still has to be evaluated and tested.

The outer field cage of the ILD TPC will be a single barrel structure serving as gas vessel and high voltage insulation. Its material budget goal is planned to be 2% X_0 at most. At the same time the wall must be thicker than the one for the inner field cage to gain sufficient mechanical robustness. A wall thickness of 60 mm, which could provide a sufficient stability, can be realized by scaling up the thickness of the honeycomb material and doubling the thickness of the GRP layers. In this case, the material budget would reach the design value of 2% X_0.

It must be stated, that the mechanical and the high voltage stability,

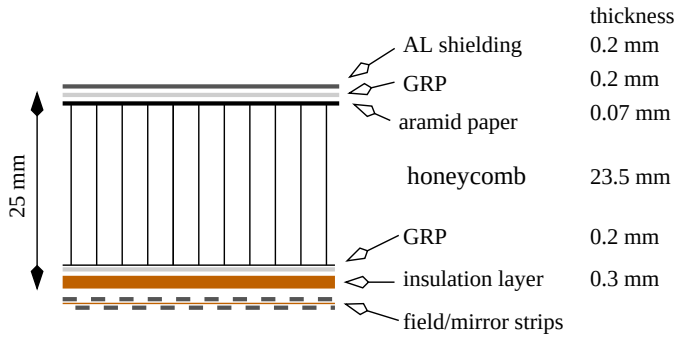

Figure 13: *First draft of the cross section for the wall of the inner field cage of the ILD TPC.*

both for the proposed inner and outer field cage wall, need to be quantified by dedicated calculations and sample piece tests. Also the precise mechanical accuracy specifications have to be revisited on the basis of further studies, also taking into account the final detector gas.

Summary

The LP is the first TPC prototype with a size relevant for a TPC of a future ILC detector. The length of the LP is 61 cm and the inner diameter of the field cage barrel of 72 cm is similar to the inner field cage for the ILD TPC.

The design of the chamber was optimized for a high electric field homogeneity of $\Delta E/E \lesssim 10^{-4}$ and a low material budget of the walls of $1.21\%\,\mathrm{X}_0$. This is close to the final design value of $1\%\,\mathrm{X}_0$. Further optimizations of the wall structure are under study and the final design goal of $1\%\,\mathrm{X}_0$ per wall seems to be in reach.

The LP is part of a test beam infrastructure which is installed at the 6-GeV DESY electron test beam. This infrastructure was realized in the framework of the EUDET project [9] and became available in November 2008. Since then it is in use by different research groups doing R&D work for a TPC of detector at a future linear collider [6].

Acknowledgments

This work is supported by the Commission of the European Communities under the 6^{th} Framework Programme 'Structuring the European Research Area', contract number RII3-026126. We thank the whole LCTPC collaboration for sharing their expertise with us in the design phase of the Large Prototype field cage. The Department of Physics of the University of Hamburg provided a valuable technical support, in particular B. Frensche, U. Pelz and the mechanical workshop. We thank the Technical University of

Hamburg-Harburg, especially P. Gührs, for the collaboration in performing the mechanical sample piece tests and the advice in the construction of the field cage.

References

[1] J. Brau *et al.* [ILC Collaboration], arXiv:0712.1950.

[2] ILD Collaboration, ILD Letter of Intent, DESY 2009-87, KEK 2009-6

[3] CERN/LHCC 2000-001, Alice TDR 7 (2000)

[4] M. Anderson *et al.*, Nucl. Instrum. Meth. A **499** (2003) 659.

[5] W. B. Atwood *et al.*, Nucl. Instrum. Meth. A **306** (1991) 446.

[6] for information see http://www.lctpc.org (2010)

[7] F. Sauli, Nucl. Instrum. Meth. A **386** (1997) 531.

[8] Y. Giomataris, P. Rebourgeard, J. P. Robert and G. Charpak, Nucl. Instrum. Meth. A **376** (1996) 29.

[9] for information see http://www.eudet.org (2010)

[10] C.K. Bowdery *et al.*, *The ALEPH Handbook: 1995*, CERN, 1995

[11] C. Amsler et al. (Particle Data Group), Physics Letters B **667**, 1 (2008) and 2009 partial update for the 2010 edition

[12] P. Schade, DESY-THESIS-2009-040